JCB Article

Multiple EphB receptor tyrosine kinases shape dendritic spines in the hippocampus

Mark Henkemeyer,[3] Olga S. Itkis,[1] Michelle Ngo,[1] Peter W. Hickmott,[2] and Iryna M. Ethell[1]

[1]Division of Biomedical Sciences and [2]Department of Psychology, University of California Riverside, Riverside, CA 92521
[3]Center for Developmental Biology and Kent Waldrep Center for Basic Research on Nerve Growth and Regeneration, University of Texas Southwestern Medical Center, Dallas, TX 75390

Here, using a genetic approach, we dissect the roles of EphB receptor tyrosine kinases in dendritic spine development. Analysis of *EphB1*, *EphB2*, and *EphB3* double and triple mutant mice lacking these receptors in different combinations indicates that all three, although to varying degrees, are involved in dendritic spine morphogenesis and synapse formation in the hippocampus. Hippocampal neurons lacking EphB expression fail to form dendritic spines in vitro and they develop abnormal spines in vivo. Defective spine formation in the mutants is associated with a drastic reduction in excitatory glutamatergic synapses and the clustering of NMDA and AMPA receptors. We show further that a kinase-defective, truncating mutation in *EphB2* also results in abnormal spine development and that ephrin-B2–mediated activation of the EphB receptors accelerates dendritic spine development. These results indicate EphB receptor cell autonomous forward signaling is responsible for dendritic spine formation and synaptic maturation in hippocampal neurons.

Introduction

The dendritic spines are characterized as small protrusions on the surface of the dendrite that receive most of the excitatory synapses (Harris, 1999) and are responsible for synaptic transmission and long-term memory. Synaptic dysfunction and pronounced deficiencies in learning and memory have been shown to be associated with abnormal spine development in various neurodevelopmental disorders, such as Rett syndrome, Down's syndrome, Angleman's syndrome, and Fragile-X syndrome (Kaufmann and Moser, 2000; Irwin et al., 2001; Fiala et al., 2002). Although our understanding of the structure and function of spine has progressed significantly, the molecular mechanisms that drive their formation and remodeling are not clear and require further investigation.

Spine development directly correlates with synaptogenesis. The initial formation of synaptic contacts between an axon and dendrite triggers spine formation and assembly of a functional cytoskeleton-signaling post-synaptic complex. The latter involves dynamic reorganization of the actin cytoskeleton that changes spine morphology from thin filopodium-like protrusions into mushroom-shaped mature spines. A number of intracellular scaffolding and signaling proteins, such as SPAR, Kalirin-7, Shank, Homer, and LIM kinase (LIMK), have been shown to induce spine morphogenesis (Pak et al., 2001; Penzes et al., 2001; Sala et al., 2001; Meng et al., 2002). Our previous data suggested that cell surface EphB receptors are the likely molecules that transduce extracellular signals into the dendrite to trigger spine morphogenesis (Ethell et al., 2001). We showed that inhibition of EphB forward signaling by the expression of dominant-negative EphB2 in cultured hippocampal neurons interfered with spine development, as judged by an absence of spines and decreased numbers of pre- and post-synaptic specializations. The role of EphB receptors (EphBs) in spine development is consistent with previous reports indicating that EphBs can be found in the post-synaptic structures of the dendrites (Torres et al., 1998; Buchert et al., 1999) and that their ephrin-B counterparts have been localized to axons (Henkemeyer et al., 1996). Furthermore, most recently, Penzes et al. (2003) have shown a connection between ephrin-B/EphB trans-synaptic signaling and the Rho-GEF Kalirin-7 in spine morphogenesis in cultured hippocampal neurons.

The online version of this article contains supplemental material.

Address correspondence to Iryna M. Ethell, Division of Biomedical Sciences, University of California Riverside, Riverside, CA 92521. Tel.: (909) 787-2186. Fax: (909) 827-7121. email: iryna.ethell@ucr.edu

Key words: dendritic spine morphogenesis; hippocampal neuron; post-synaptic; receptor signaling; synapse

Abbreviations used in this paper: AMPAR, AMPA receptor; DIV, days in vitro; GABA, γ-aminobutyric acid; GAD, glutamic acid decarboxylase; GluR, glutamate receptor; IR, immunoreactivity; KO, knockout; LIMK, LIM kinase; NMDAR, NMDA receptor; PSD, post-synaptic density; WT, wild type.

The Journal of Cell Biology, Volume 163, Number 6, December 22, 2003 1313–1326
http://www.jcb.org/cgi/doi/10.1083/jcb.200306033

The Journal of Cell Biology

The Eph family forms the largest group of receptor tyrosine kinases that interact with membrane-anchored ligands known as ephrins (Pasquale, 1997; Flanagan and Vanderhaeghen, 1998; Kullander and Klein, 2002). Upon stimulation by ephrin ligands, Eph receptors activate signaling cascades in various biological systems. Interactions between Ephs and ephrins are implicated in repulsive axon guidance, cell migration, topographic mapping, and angiogenesis (for reviews see Flanagan and Vanderhaeghen, 1998; Kullander and Klein, 2002). Besides their functions in development, Ephs and Ephrins are implicated in the regulation of NMDA-dependent synaptic function in mature synapses. Dalva et al. (2000) have shown EphB2 involvement in NMDA receptor (NMDAR) clustering and recruitment of the NMDAR to post-synaptic specialization. Moreover, Grunwald et al. (2001) and Henderson et al. (2001) have confirmed that EphB activation modulates synaptic plasticity in cultured hippocampal neurons through regulation of NMDAR-activated pathways. The expression of EphB2 is regulated in an activity-dependent manner by stimuli known to induce synaptic plasticity, and mice lacking EphB2 display defects in synaptic plasticity. However, EphB2 mice are viable and show normal synapse and spine morphology in CA1 (Grunwald et al., 2001). At least four members of the Eph receptor family, EphB1, EphB2, EphB3, and EphA4, are found in the hippocampus (Liebl et al., 2003) and show some overlapping expression. This suggests that the appearance of relatively normal synapses in the EphB2 single mutants reported by Grunwald et al. (2001) is likely due to counterbalance by the coexpressed EphB1, EphB3, or EphA4.

Here, using a genetic approach, we dissect the roles of the different EphBs in spine development in vitro and in vivo. Analysis of double and triple knockout (KO) mice lacking EphB1, EphB2, and EphB3 in different combinations indicates that all these EphBs, although to varying degrees, are responsible for spine morphogenesis and synapse formation in the hippocampus. Hippocampal neurons in triple *EphB1, EphB2, EphB3*-deficient mice fail to form spines in vitro and develop abnormal spines in vivo. Analysis of the single and double EphB-deficient mice in various combinations indicates that the EphB1 and EphB2 are the main players in shaping spines in hippocampal neurons in vitro. We show further that the mutant mice expressing a truncated form of the EphB2 lacking the cytoplasmic domain also show spine abnormalities, indicating that EphB forward signaling is responsible for normal spine formation.

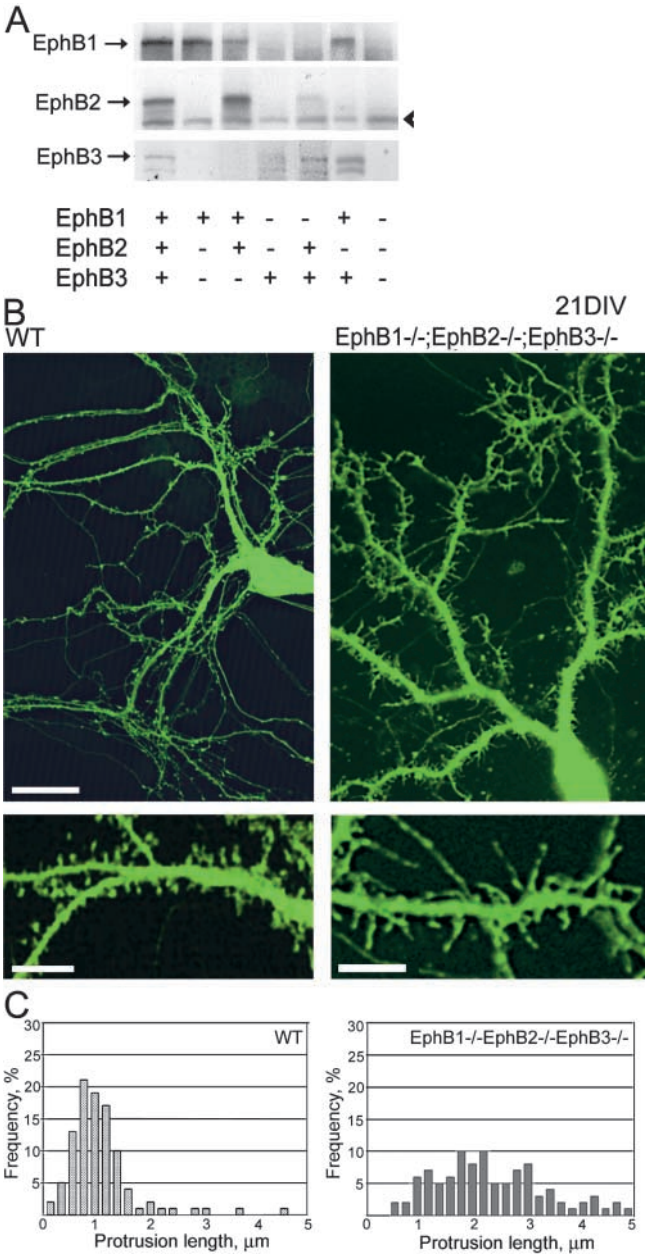

Figure 1. **The spine morphogenesis in cultured hippocampal neurons is failed in absence of the EphB receptors.** (A) Expression of EphB1, EphB2, and EphB3 in cultured hippocampal neurons from the various combinations of EphB KOs by Western blot analysis. (B) Morphology of GFP-labeled spines in 21 DIV–cultured hippocampal neurons from WT and triple EphB-deficient (EphB1−/−,EphB2−/−, EphB3−/−) mice. The hippocampal neurons were transfected with GFP at 7 DIV and examined at 21 DIV. Bars: (top) 10 μm; (bottom) 2 μm. (C) Quantitative analysis of the lengths of dendritic protrusions ($n > 500$).

Results

Triple EphB-deficient hippocampal neurons fail to make dendritic spines in vitro

To determine the roles of different EphBs in formation of spines and synapses, we looked at spine development in cultured hippocampal neurons that lacked three EphB receptors, EphB1, EphB2, and EphB3. We generated compound triple homozygotes using a newly generated protein-null mutation in the *EphB1* gene (Williams et al., 2003), and preexisting null mutations in *EphB2* (Henkemeyer et al., 1996) and *EphB3* (Orioli et al., 1996). The adult mice that are triple homozygous null mutant for all three of these related genes were viable and able to breed.

Hippocampal neurons were isolated from embryonic day 15–16 embryos of triple *EphB* mutants and wild-type (WT) mice, and maintained in cultures for 3–4 wk. Spines in cultured WT hippocampal neurons are observed to form between 7 and 14 d in vitro (DIV). By 14 DIV, most dendritic protrusions are spines, however, their maturation continues

until 21 DIV. Spine morphogenesis in WT cultures is characterized by a decrease in spine length and formation of mature mushroom-like shapes that contain polymerized F-actin (Ethell and Yamaguchi, 1999). The analyses of spine morphogenesis in hippocampal neuron cultures from the triple EphB-deficient (KO) neurons failed to detect spines even at 21 DIV (Fig. 1). Although most spines in WT neurons at 21 DIV are mushroom-shaped short protrusions with polymerized F-actin, protrusions in KO neurons are long, thin, and immature, without F-actin clusters (Fig. 2 A). Although, F-actin polymerization was not seen on the protrusions in KO neurons, rhodamine-coupled phalloidin-positive puncta was seen in the dendritic shaft, often at the base of the filopodia. Therefore, in KO neurons phalloidin labeling indicated actin polymerization but not formation of mature spines. The data suggest that targeting of the branched actin network to protrusions was affected rather than the actual process of actin polymerization into mesh-like networks.

The morphological formation and maturation of spines in normal cultured hippocampal neurons directly correlates with synapse formation (Ethell and Yamaguchi, 1999). Most excitatory (glutamatergic) synapses in the hippocampus are formed on spines. If the KO neurons don't make spines, do they make synapses? To analyze synapse formation in these neurons, we examined the distribution of pre- and post-synaptic proteins such as synaptophysin and PSD-95, respectively. Positive synaptophysin and PSD-95 immunoreactivities (IRs) were detected in both WT and KO neurons (Fig. 2, B and C). However, the distributions of synaptophysin and PSD-95 clusters were different. In the KO neurons, the synaptophysin-positive boutons were larger and localized directly on the dendritic shaft rather than on protrusions (Fig. 2 B). A quantitative analysis showed that the changes in the size of the synaptophysin-positive boutons in vitro with $0.37 \pm 0.11\ \mu m^2$ in KO and $0.26 \pm 0.09\ \mu m^2$ in WT neurons were statistically significant. This is not surprising as presynaptic boutons of symmetric shaft synapses are usually larger in size then presynaptic terminals of asymmetric spine synapses. Most of the PSD-95 clusters in KOs were also identified on the dendritic shaft, whereas the PSD-95–positive post-synaptic sites in WT neurons were mainly localized on the spines (Fig. 2 C). Moreover, the PSD-95 clusters in mutants were smaller than in the WT cultures with $0.20 \pm 0.07\ \mu m^2$ in KO and $0.28 \pm 0.14\ \mu m^2$ in WT neurons. Western blot analysis showed that only a small portion of PSD-95 was fractionated in crude synaptosome fraction in cultures of KO neurons and was not detected in the synaptic membrane fraction (Fig. 2 F). Although in WT cultures PSD-95 was fractionated into the crude synaptosome fraction and further enriched in the synaptic membrane fraction. The synaptic vesicle marker, synaptophysin, was present in the crude synaptosome fraction of both WT and KO neurons.

Therefore, protrusions in WT cultures that showed mushroom-like mature spines and contained polymerized F-actin also formed synapses with PSD-95 clusters and synaptophysin-positive presynaptic boutons. Dendritic protrusions in triple EphB-deficient neurons, which were long, thin, and had filopodia-like morphology, did not contain F-actin clusters and lacked synaptic inputs. These results demonstrate that in culture, the EphBs are necessary for formation of spines as morphological domains and synaptic targets.

EphB receptors are necessary for glutamatergic but not γ-aminobutyric acid (GABA)ergic synapse formation in cultured hippocampal neurons

Although the triple EphB-deficient hippocampal neurons failed to make spine synapses, the formation of shaft synapses was not disturbed. Dendritic spines usually receive most of the excitatory synapses in hippocampal neurons. To determine whether an absence of spines in KO neurons reflect a failure to form excitatory synapses, we examined the localization of excitatory glutamatergic and inhibitory GABAergic synapses in these neurons. We used immunodetection of NMDA and AMPA receptors (AMPARs) to localize glutamatergic synapses and glutamic acid decarboxylase (GAD) as a marker for presynaptic boutons of inhibitory GABAergic synapses. The overall NMDAR2A/B and glutamate receptor (GluR)2 IRs were greatly reduced in KO neurons; no visible clusters were detected on dendritic filopodia or the dendritic shaft (Fig. 2 D). The results were similar to what we have seen in neurons that overexpressed the kiEphB2 receptor, whereas kinase activities of the EphBs were inhibited (Ethell et al., 2001). Although in WT neurons, numerous NMDAR2A/B and GluR2-immunoreactive clusters were observed along dendrites, many of which were colocalized with spine heads (Fig. 2 D). Western blot analysis also showed that overall level of NMDAR and GluR2 in cell lysates of KO neurons decreased compared with that in WTs. Moreover, NMDAR2A/B and GluR2 were not detected in crude synaptosome or synaptic membrane fractions of KOs, whereas in WT cultures, fractionation patterns for NMDAR2A/B and GluR2 were similar to that of PSD-95 (Fig. 2 F). Immunostaining for the GABAergic synapse marker GAD showed that the formation of GABAergic synapses on the dendritic shaft was not affected in KO neurons (Fig. 2 E). Lack of GluRs in synaptosome fraction, their diffuse cluster-free distribution, and a positive staining for GAD suggest that most synapses formed on the dendritic shaft in triple EphB-deficient neurons are GABAergic. These data show that the EphBs are involved in both spine morphogenesis and glutamatergic synapse formation.

The EphB receptors act as a team

To determine which of the EphBs, EphB1, EphB2, or EphB3, is responsible for the effect on spine formation, we analyzed all the various combinations of *EphB* mutants. The cultured hippocampal neurons from single (*EphB1, EphB2*, or *EphB3*) and double (*EphB1*/*EphB2*, *EphB1*/*EphB3,* or *EphB2*/*EphB3*) mutants were analyzed over 21 DIV for morphologic features (by GFP fluorescence), F-actin polymerization (phalloidin staining), and synapse formation (immunostaining for pre- and post-synaptic markers). The single mutants developed mature, mushroom-shaped spines similar to WT neurons (Fig. 3 A). There were no significant differences in spine length or shape, F-actin polymerization and number of pre- and post-synaptic sites (Fig. 3 B).

The neurons from double mutants showed obvious defects in spine formation. The spines were longer and more

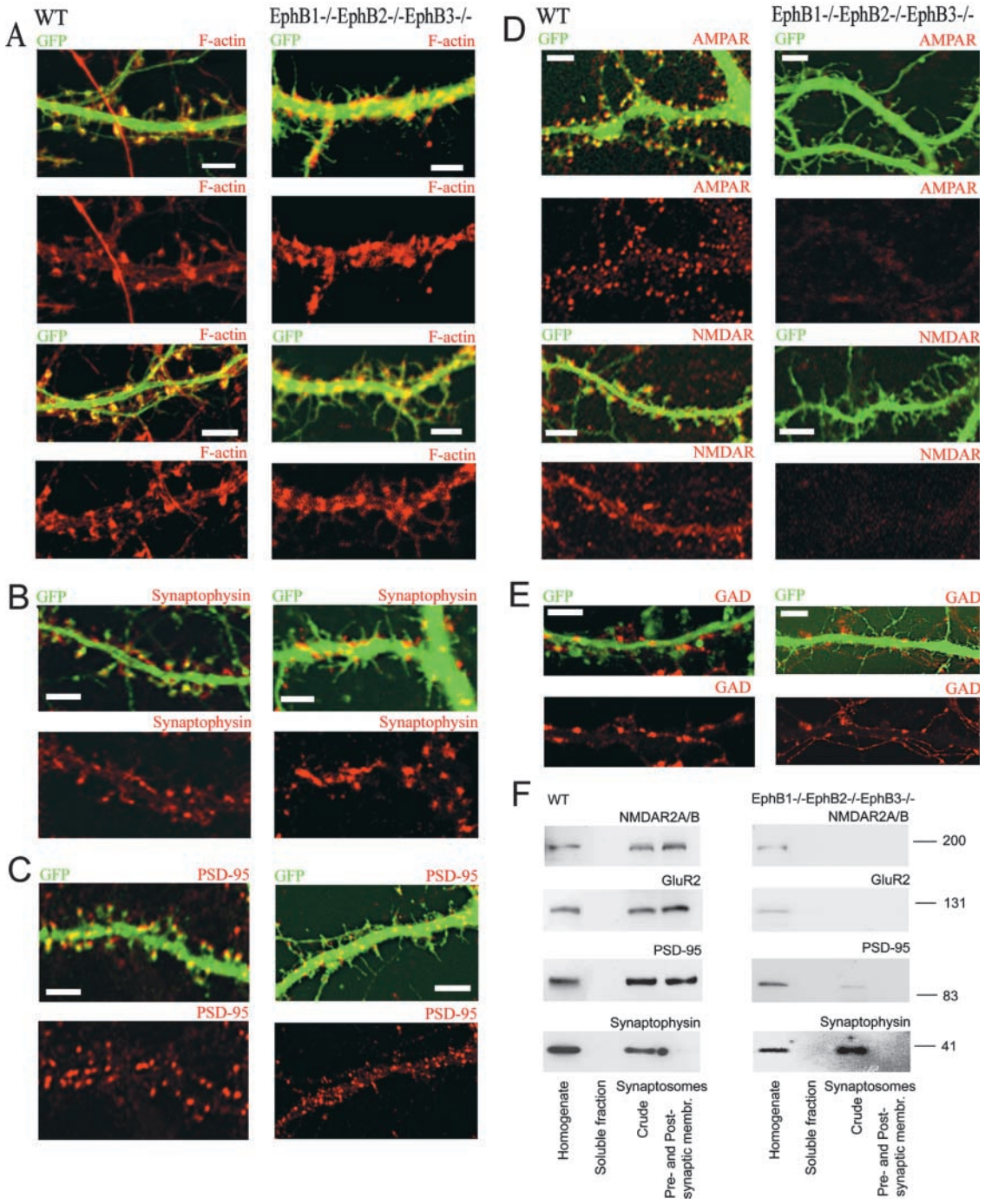

Figure 2. **Triple EphB-deficient neurons fail to make spine synapses in cultures.** Cultured hippocampal neurons from WT and triple EphB-deficient (EphB1−/−,EphB2−/−,EphB3−/−) mice were transfected with GFP at 7 DIV and examined at 21 DIV. (A) Detection of polymerized F-actin by rhodamine-coupled phalloidin. Confocal images of GFP fluorescence (green) and rhodamine-coupled phalloidin (red). (B) Immunodetection of synaptophysin-positive presynaptic boutons. Confocal images of GFP fluorescence (green) and anti-synaptophysin IR (red). (C) Analysis of the distribution of post-synaptic sites by immunodetection of post-synaptic protein PSD-95. Confocal images of GFP fluorescence (green) and anti–PSD-95 IR (red). (D) Detection of glutamatergic synapses by immunostaining with anti-GluR2 and NMDAR2A/B antibodies. Confocal images of GFP fluorescence (green) and anti-GluR2 (AMPAR) or anti-NMDAR2A/B (NMDAR) IRs (red). (E) Detection of GABAergic synapses by immunostaining for GAD. Confocal images of GFP fluorescence (green) and anti-GAD65 IR (red). (F) Western blot analysis of subcellular distribution of NMDAR2A/B, GluR2, PSD-95 and synaptophysin in WT (left) and triple EphB1−/−EphB2−/−EphB3−/− (right) hippocampal neurons at 21 DIV. Subcellular fractionations were prepared as described in Materials and methods. Bars, 1 μm.

variable in length than those from WT neurons (Fig. 3 B). The number of mature mushroom-like spines significantly decreased in the double mutants, whereas the proportion of filopodia-like protrusions increased as compared with WT or single KO neurons. Interestingly, the EphB1/EphB2-deficient neurons showed the most pronounced defects in spine formation that were similar to the triple mutants. The protrusions in EphB1/EphB2-deficient neurons

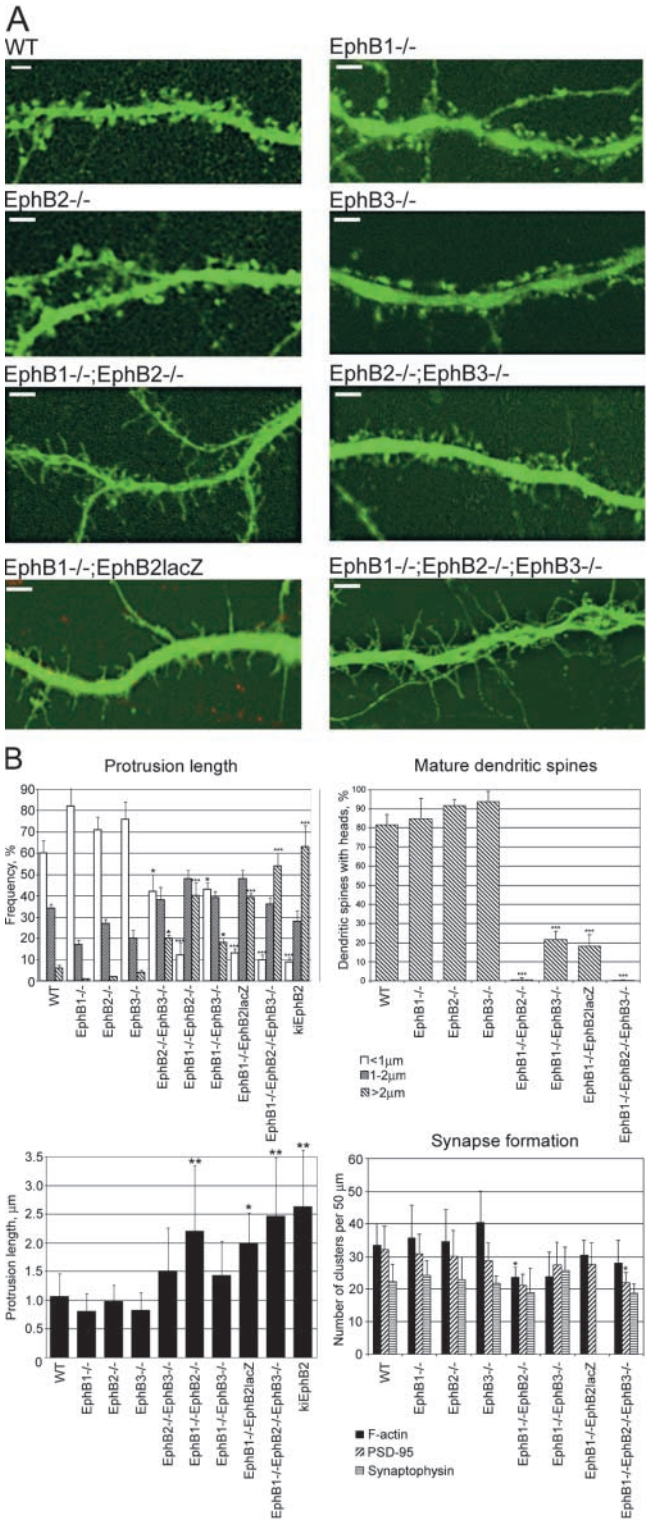

Figure 3. **The EphB1 and EphB2 receptors are main contributors to spine morphogenesis in the cultured hippocampal neurons.** Analysis of spine morphogenesis in cultured hippocampal neurons from WT and EphB-deficient mice: single EphB KOs (EphB1−/−, EphB2−/−, or EphB3−/−); double EphB KOs (EphB1−/−;EphB2−/−, or EphB2−/−;EphB3−/−); triple EphB KO (EphB1−/−;EphB2−/−; EphB3−/−), or double mutants that express a truncated form of the EphB2 (EphB1−/−;EphB2lacZ). The cultured hippocampal neurons were transfected with GFP at 7 DIV. Spine morphology was examined at 21 DIV. (A) Confocal images of GFP-labeled spines in 21 DIV–cultured hippocampal neurons with various EphB KOs. Bars, 1 μm. (B) Quantifications of spine morphogenesis and synapses in 21 DIV–cultured hippocampal neurons with various EphB KOs. The spine morphogenesis was assayed by analysis of spine lengths (left; $n > 500$), percent of mature mushroom-like spines relative to total number of protrusions (right, top). Synapse formation was analyzed by numbers of synaptophysin-positive and PSD-95–positive IRs (right, bottom). Error bars indicate SD. *, $P < 0.05$; **, $P < 0.001$; ***, $P < 0.0001$ with *t* test.

were long, thin filopodia-like protrusions without heads and polymerized F-actin (Fig. 3). The analysis of synapse formation by immunostaining for pre- and post-synaptic proteins, such as synaptophysin and PSD-95, showed only a modest decrease in the number of synapses in EphB1/EphB2-deficient neurons compared with WT neurons (Fig. 3 B). However, similar to triple EphB-deficient neurons, the distribution of synaptophysin and PSD-95 clusters indicated formation of shaft synapses instead of spine synapses in the EphB1/EphB2 double mutants. Although hippocampal neurons from EphB2/EphB3 and EphB1/EphB3 double mutants showed a decreased number of mature spines and spine synapses, they nevertheless were able to make spines. However, the EphB1/EphB2-deficient neurons, similar to triple EphB-deficient ones, failed to make spines in vitro. Thus, multiple EphBs appear to share control over spines in culture, with the most significant contribution of the EphB1 and EphB2 receptors.

Ephrin-B/EphB receptor signaling: axon–dendritic course in cultured hippocampal neurons

The different EphBs show distinct expression patterns in the hippocampus. In the neonatal hippocampus, CA1 pyramidal neurons preferentially express EphB2 and EphB3, whereas CA3 neurons express EphB1 and EphB2 (Liebl et al., 2003). To determine the complement of EphBs present in the cultured WT hippocampal neurons, the cultures were immunostained with specific anti-EphB1, anti-EphB2, and anti-EphB3 antibodies (Fig. 4 A). All three receptors appear to be expressed on dendrites of WT hippocampal neurons and show puncta-like distribution in mature 21 DIV cultures (Fig. 4 A). Moreover, there were no distinct populations of EphB3- or EphB1-positive neurons in vitro. The EphB1 and EphB2, or EphB2 and EphB3 double immunostaining showed partial colocalization of the receptors (Fig. 4).

Interestingly, although differences in the expression of EphBs between CA1 and CA3 neurons are lost in culture, the ephrin-B expression detected by a pan-ephrin-B antibody remains specific to some neurons but not others. Ephrin-B–positive neurons (~35%) showed strong immunolabeling in axons, with weaker puncta-like IR in cell bodies and on dendrites that colocalized with synaptophysin-positive axon terminals (Fig. 4 B). The ephrin-B expression appears to be restricted to axons of granular-shaped neurons rather then pyramidal neurons. Moreover, double immunostaining with anti-EphB2 and pan-ephrin-B–specific antibodies showed localization of EphB2-positive clusters in close proximity to ephrin-B–positive IRs, but no overlap (Fig. 4 C). This data suggest that ephrin-B/EphB signaling controls spine formation in cultured hippocampal neurons primarily by axon–dendritic cross-talk.

Ephrin-B–mediated activation of EphB receptors accelerates spine morphogenesis in vitro

Because loss of EphB1 and EphB2 expression blocked spine formation in cultured hippocampal neurons, we tested whether spine formation can be accelerated by ligand-mediated activation of the EphBs. A soluble preclustered form of the ephrin-B2 (ephrin-B2-Fc chimera) was used to cluster and activate EphBs in 7–14 DIV hippocampal neurons (Gerlai, 2000).

We used GFP fluorescence to visualize protrusions in cultured WT hippocampal neurons after 7 or 14 DIV and monitor their morphologic features after the application of 2 μg/ml preclustered ephrin-B2-Fc. Application of ephrin-B2-Fc to WT cultures resulted in a reduced number filopodia-like protrusions and an increased number of spines at 7 and 14 DIV (Fig. 5; see Fig. S1, available at http://www.jcb.org/cgi/content/full/jcb.200306033/DC1). The proportion of filopodia was significantly reduced, from 35 ± 3% to 14 ± 3.5%.

Moreover, ephrin-B2-Fc also induced spine maturation in 14 DIV cultures as spines became shorter and had bigger heads (Fig. 5 D). The average length of spines was reduced from 1.56 ± 0.38 μm in the Fc controls to 1.34 ± 0.24 μm in ephrin-B2-Fc–induced cultures. The spine heads were larger after ephrin-B2-Fc treatment with average head area of 0.32 ± 0.06 μm^2 compared with 0.18 ± 0.04 μm^2 in control Fc-treated cultures.

To confirm that observed changes were due to ephrinB2-Fc induced activation of EphBs, we assayed whether ephrin-B2-Fc application induced EphB2 clustering and autophosphorylation in WT neurons. Indeed, ephrin-B2-Fc application induced both activities (Fig. 5, A, B, and F). Western blot analysis showed significant increase in tyrosine phosphorylation of the EphB2 15 min after ephrin-B2-Fc application (Fig. 5 B). Immunostaining of the cultures with specific anti-EphB2 antibody detected multiple EphB2 clusters along dendrites of the neurons, on spines, and on the dendritic shaft (Fig. 5, A and F).

Therefore, morphologic transformation of filopodia-like protrusions into spines in cultured WT hippocampal neurons induced by ephrin-B2-Fc was primarily due to activation of EphB forward signaling.

Dendritic spine development is impaired in hippocampal neurons of triple EphB-deficient neurons in vivo

The analyses of spines in the hippocampi of the triple EphB mutant (KO) mice show a significant decrease in spine density and formation of abnormal headless or small-headed spines.

The spines in hippocampal slices were visualized by filling individual pyramidal neurons with biocytin. This revealed that the density of the spines was significantly reduced in KO neurons to 12.52 ± 2.51 spines per 100 μm of dendrite versus 46.71 ± 1.55 in WT neurons, whereas the dendritic arborization was normal (Fig. 6). Morphology of the spines that did form in KO neurons was also abnormal. The most pronounced abnormalities were seen in CA3 neurons. Although most of the spines in WT CA3 neurons are mushroom-shaped (thin neck and large head), spines in KO CA3 neurons have very small or no heads (Fig. 6). Moreover, EM analyses

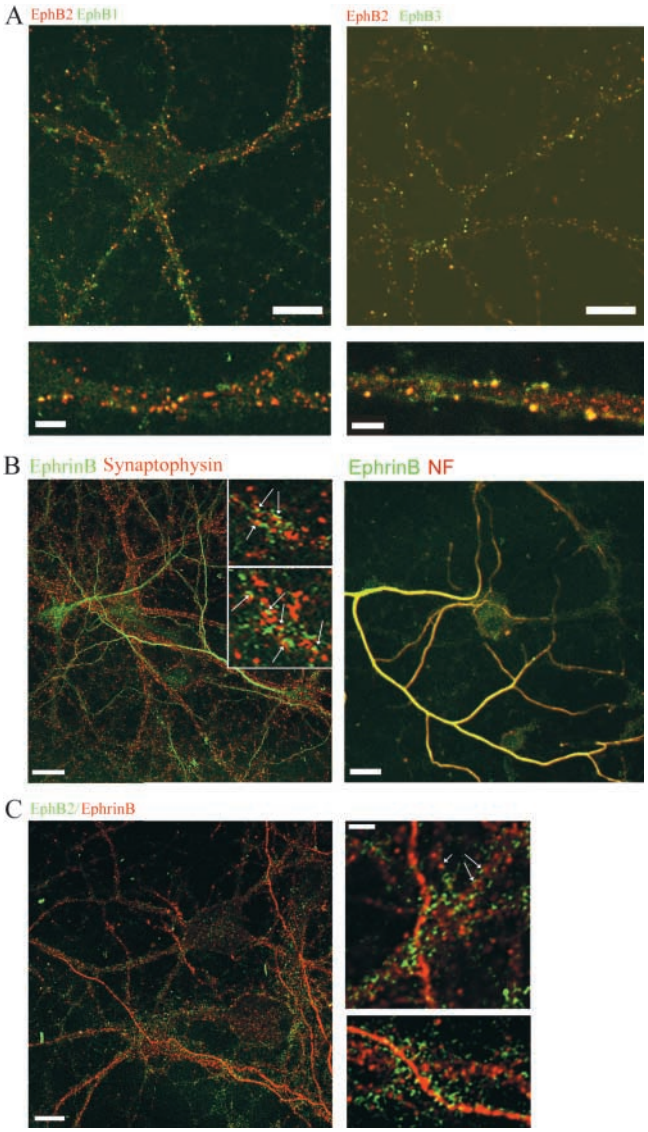

Figure 4. **Distribution of ephrin B and EphB receptors in cultured hippocampal neurons.** (A) Immunodetection of EphB1, EphB2, and EphB3 in 21 DIV–cultured hippocampal neurons. Confocal images show partial colocalization of the EphB1 and EphB2 or EphB2 and EphB3 IRs (yellow). Bars: (top) 10 μm; (bottom) 1 μm. (B) Double immunolabeling of 21 DIV–cultured hippocampal neurons with anti–pan-ephrin-B (green) and anti-synaptophysin (left, red) or anti-NF antibody (right, red). The confocal analysis show axon-specific localization of the B-class ephrins. Bars, 10 μm. The examples of juxtaposition of synaptophysin and ephrin-B are indicated by arrows. (C) B-class ephrins (red) and EphB2 (green) IRs are localized in close proximity, but do not overlap (no yellow, arrows). Bars: (left) 10 μm; (right) 1 μm.

of ultrathin section of hippocampal CA3 area reveal a significant reduction in cross-sectional area of the post-synaptic component of asymmetric synapses (post-synaptic area) from 0.12 ± 0.06 μm^2 in WTs to 0.06 ± 0.02 μm^2 in triple KOs (see Fig. 8, B and C). The length of the post-synaptic density (PSD) was also significantly reduced from 0.33 ± 0.08 μm in WTs to 0.23 ± 0.06 μm in KOs (see Fig. 8 C). These data are consistent with the small head size observed in biocytin-filled neurons (Fig. 6). The EM analysis also shows a de-

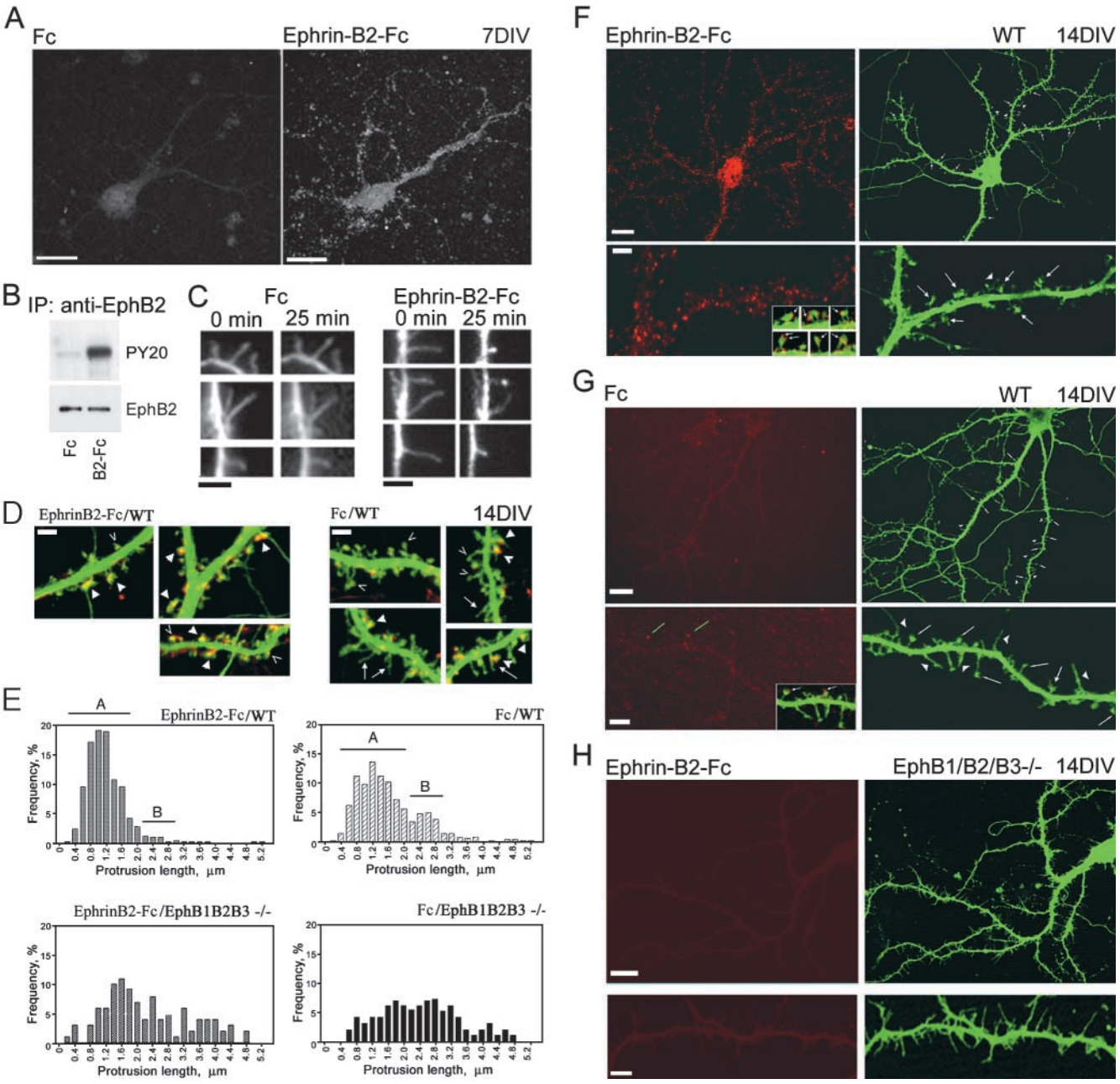

Figure 5. **Clustered ephrin-B2-Fc promotes spine morphogenesis in cultured hippocampal neurons.** Clustered ephrin-B2-Fc or control Fc was applied to cultured GFP-expressing hippocampal neurons at (A–C) 7 DIV or (D–H) 14 DIV. (A) Immunodetection of EphB2 in 7 DIV–cultured hippocampal neurons after treatment with control Fc (left) or EphrinB2-Fc (right). Clustered ephrin-B2-Fc induced clustering of the EphB2. Bars, 10 μm. (B) Autophosphorylation of EphB2 is induced by ephrin-B2-Fc treatment as shown by Western blot. (C) Live images of GFP-labeled dendritic protrusions in 7 DIV WT hippocampal neurons after treatment with ephrin-B2-Fc, or Fc at 0 and 25 min. Bars, 1 μm. (D) Confocal images of spines in GFP-labeled 14 DIV WT hippocampal neurons treated with ephrin-B2-Fc (left) or control Fc (right) for 4 h. The spines are visualized by GFP fluorescence (green) and actin polymerization (red) by staining for F-actin with rhodamine-coupled phalloidin. Filopodia are indicated by arrows; spines with smaller heads are indicated by open arrowhead; and spines with large heads are indicated by closed arrowheads. Bars, 1 μm. (E) Quantitative analysis of the lengths of dendritic protrusions in 14 DIV–cultured hippocampal neurons, WT (top) or triple EphB-deficient (EphB1B2B3−/−, bottom), treated with ephrin-B2-Fc (left) or control Fc (right). Group A represents spines and group B represents dendritic filopodia ($n > 500$). Note: Clustered ephrin-B2-Fc induced elimination of dendritic filopodia and increased spine number in 14 DIV–cultured hippocampal neurons from WT mice, but not in triple EphB-deficient hippocampal neurons. (F–H) Confocal images of spines in GFP-labeled 14 DIV WT hippocampal neurons treated with ephrin-B2-Fc (F) or control Fc (G), and triple EphB1,B2,B3 KOs hippocampal neurons treated with ephrin-B2-Fc (H). Bars: (top) 10 μm; (bottom) 1 μm. (F) Clustered ephrin-B2-Fc induced mature mushroom-like morphology and EphB2 clustering in WT 14 DIV–cultured hippocampal neurons. The cultures are analyzed for spine morphology by GFP fluorescence (green) and for EphB2 clusters by immunostaining using anti-EphB2 antibody (red). Note: The spines with bigger heads (arrows), which were induced by ephrin-B2-Fc, showed EphB2 clusters (red, high magnification insert). (G) Control Fc treated cultures show only few EphB2 clusters (red, arrows) that are typical for hippocampal neurons at 14 DIV. (F and G) Filopodia are indicated by arrowheads; spines are indicated by arrows. (H) Clustered ephrin-B2-Fc does not induce mushroom-like morphology in triple EphB-deficient 14 DIV hippocampal neurons (EphB1B2B2−/−). The EphB2 IR is not detected.

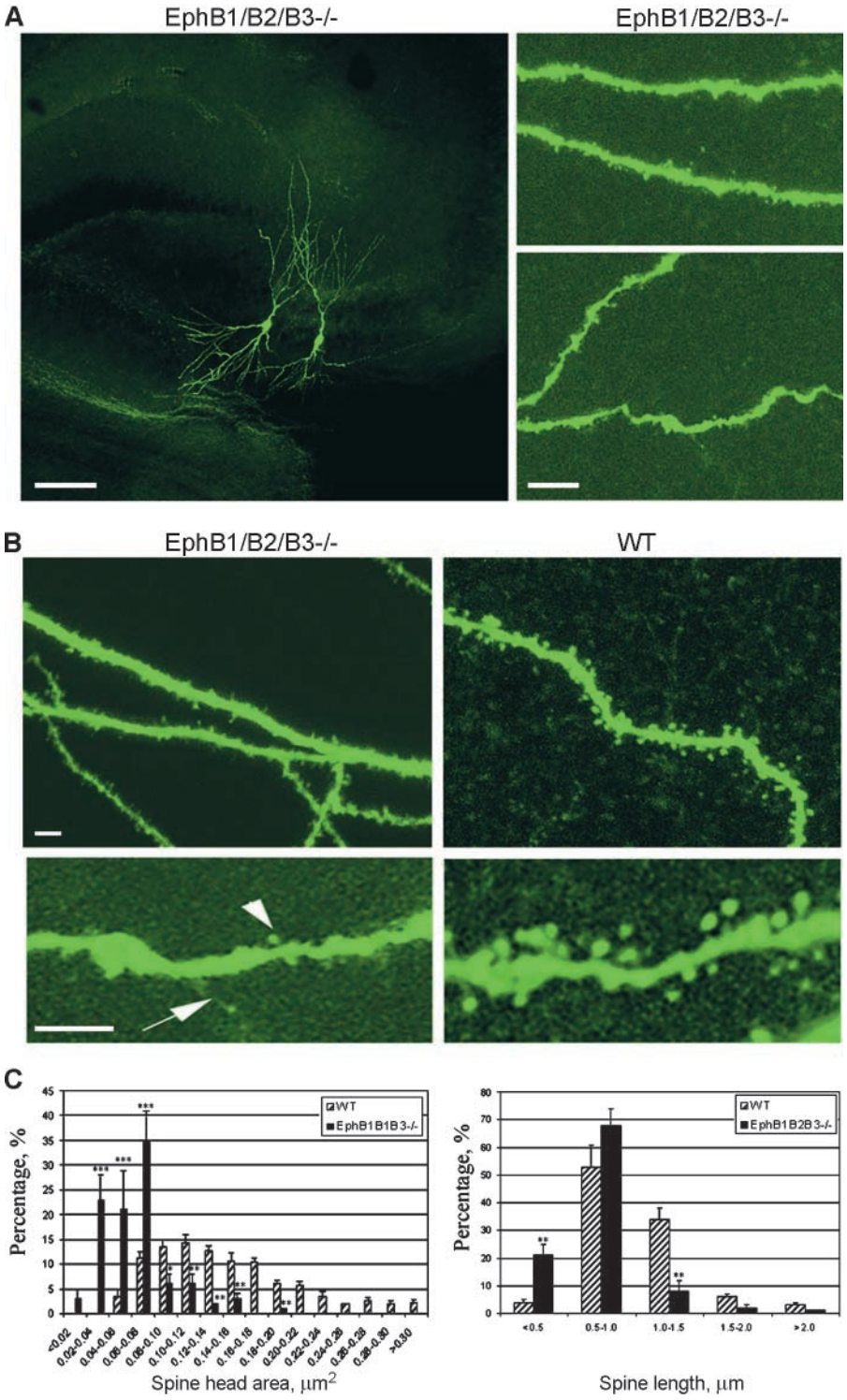

Figure 6. **Spines in hippocampi of triple EphB-deficient mice reveal abnormal headless or small-headed morphology.** (A) A projection of a 3-D reconstructed confocal image of biocytin-filled CA3 pyramidal cell pair from hippocampus of the triple EphB-deficient (EphB1B2B3−/−) mice (left). (Right) High magnification view shows dendrites and spines. Bars: (left) 100 μm; (right) 10 μm. (B) Morphology of spines in biocytin-filled CA3 neurons of hippocampal slices from triple EphB-deficient (EphB1B2B3−/−) and WT mice. There are fewer spines are found in triple EphB-deficient neurons as compared with WT. The spines in EphB-deficient neurons exhibit headless (arrow) or small-headed morphology (arrowhead), whereas in WT neurons spines reveal mature mushroom-like morphology with bulbous heads and thin necks (right). Bars, 2 μm. (C) Quantification of spine head area (left) and spine lengths (right) in triple EphB-deficient (EphB1B2B3−/−) and WT hippocampus ($n > 300$ for each mice). Error bars indicate SD. *, $P < 0.05$; **, $P < 0.001$; ***, $P < 0.0001$ with *t* test. (D and E) Immunohistochemical localization of (D) PSD-95 and (E) synaptophysin in stratum lucidum (SL) and stratum radiatum (SR) of hippocampi in the triple EphB-deficient (EphB1/B2/B3) and WT mice (WT). SP, stratum pyramidale. Bars, 50 μm.

creased number of asymmetric synapses (spines) and increased number of symmetric synapses on dendritic shaft in triple KOs (EphB1B2B3−/−) as compared with WTs (see Fig. 8 A). It was also noted that the dendritic surface free of synaptic contact is completely ensheathed by astrocytic processes.

To determine whether multiple EphBs are responsible for spine development in hippocampus in vivo, we performed in vivo analysis of the spine morphology and synapse ultrastructure in hippocampi of EphB1/EphB2 and EphB2/EphB3 double mutants. The EphB1/EphB2 mutants showed abnormal headless spines in CA3 pyramidal neurons as did the triple EphB mutants (Fig. 7). However, the CA1 pyramidal neurons showed normal spine morphology in the EphB1/EphB2 mutants, which suggest involvement of the EphB3 in shaping spines in CA1 hippocampi, as the EphB3 is shown to be preferentially expressed in CA1 pyramidal neurons. Furthermore, the KO of all three EphBs affected development of spines in CA1 pyramidal neurons (Fig. 7). Therefore, multiple EphBs are responsible for spine formation in hippocampal neurons in vivo.

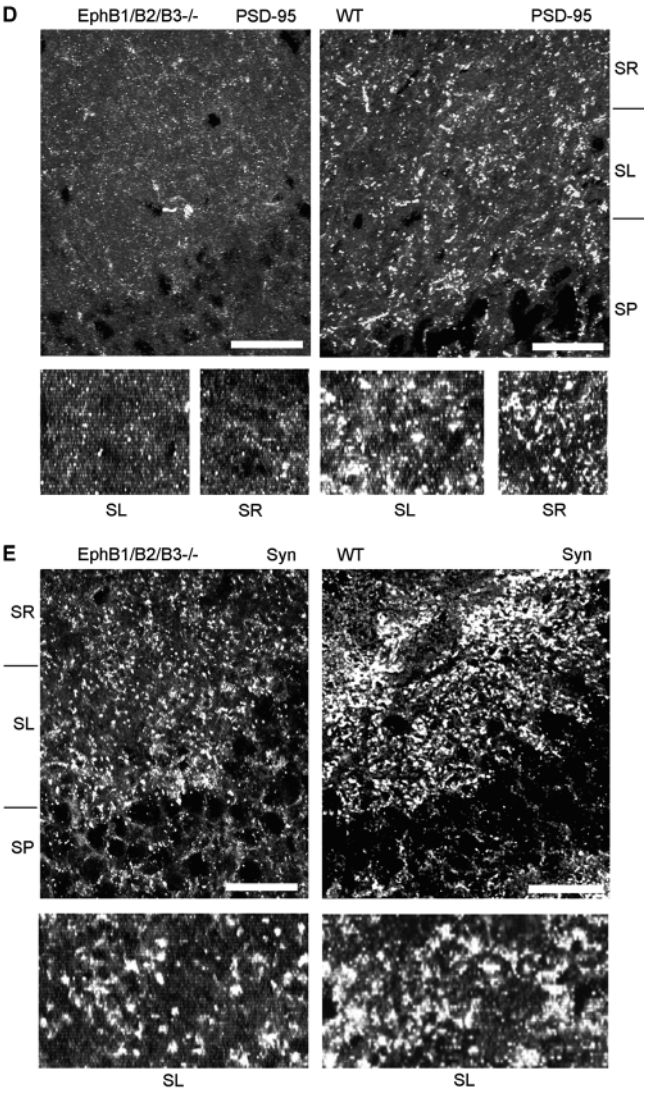

EphB forward signaling is important for normal spine formation in hippocampal neurons

A total absence of EphBs in the triple EphB-deficient hippocampal neurons would also interfere with possible noncell autonomous functions in which the receptors can also act as ligands to activate reverse signaling in ephrin-B–expressing cells (for review see Cowan and Henkemeyer, 2002). To determine whether the function of EphB2 in hippocampal spines involves cell autonomous forward signaling or nonautonomous reverse signaling, we generated EphB1/EphB2 double mutants using the previously described *EphB2*^{lacZ} allele (Henkemeyer et al., 1996). This mutation leads to the expression under the endogenous promoter/enhancer elements of a truncated, membrane-anchored EphB2-βgal fusion protein lacking the majority of its cytoplasmic domain, including the tyrosine kinase domain and the COOH-terminal PDZ domain binding site. Although, the EphB2-βgal fusion protein cannot transduce cell autonomous forward signals, the EphB2 extracellular and transmembrane domains are still present and thus can still function as a ligand to bind ephrin-B molecules and activate reverse signaling. In the hippocampal neuron cultures as well as in vivo, we found defective spine development using the *EphB2*^{lacZ} allele that was similar to the results obtained with the EphB2 protein-null allele (Figs. 3 and 7). Thus, this data indicates that EphB2 forward signaling is important for normal spine formation in hippocampal neurons.

Discussion

Here, we show that EphBs play a critical role in spine development in vitro and in vivo using the power of a genetic approach. The EphB1-, EphB2-, and EphB3-deficient neurons in various single, double, and triple combinations allowed us to dissect the role of the different EphBs in spine formation in hippocampal neurons. We show that multiple EphBs are involved in shaping dendritic spines in cultured hippocampal neurons with the EphB1 and EphB2 as the main players. Our data support the idea that axon–dendritic cross-talk of the ephrin-B/EphB molecules direct spine formation. They also indicate that the EphBs not only control spine formation but also induce mature spine morphology and mature synapses containing NMDA and AMPARs. Few spines that form in the hippocampi of triple EphB-deficient neurons in vivo have immature, headless morphology. Moreover, Ephrin-B2–mediated activation of the EphBs in vitro transforms thin immature spines into mature forms with spacious spine heads. Altogether, our data demonstrate that EphB forward signaling is responsible for normal spine development in hippocampal neurons, with the contribution of the multiple EphBs.

The EphB versus EphA receptors in the hippocampus

Both, in vitro and in vivo data show that the EphBs play an important role in spine formation in hippocampal neurons. However, in vivo, spine formation has not completely failed. Why is the effect of triple EphB deletion more striking in vitro than in vivo? Besides the EphBs, the EphA4 is also expressed in the hippocampus. Murai et al. (2003) recently showed that a repulsive interaction between the EphA4 and its ligand ephrin-A3 is involved in the regulation of spine formation in the hippocampus. Although ephrin-B/EphB signaling regulates synaptic structure in an axo–dendritic direction, the ephrin-A/EphA4 interaction appears to involve glial–dendritic communication. In primary hippocampal neuron cultures, the proportion of glial cells is much lower (~5%) than that in vivo. Therefore, in culture, glia-dendritic cross-talk has little or no effect on the regulation of spines, and the interaction between ephrin-B and EphB is primarily responsible for the formation and maintenance of post-synaptic structures (Fig. 9).

In vivo, glial cells play an important role in stabilizing spines. In mature hippocampi, astrocytes completely enwrap dendrites and axons to shield synapses from each other (Fig. 8 A). The astrocytic shielding also prevents the extension of many new filopodia in mature hippocampi and enhances the stability of existing spines. Recent data suggest that the transient interaction between ephrin-A and EphA4 underlies the glial-dependent stabilization of spines (Murai et al., 2003); whereas our data suggest that the ephrin-B/EphB signaling is primarily responsible for the formation of spines and its maintenance in an axo–dendritic direction.

There are fewer spines in triple EphB-deficient neurons in vivo and more synapses are formed on dendritic shafts as ob-

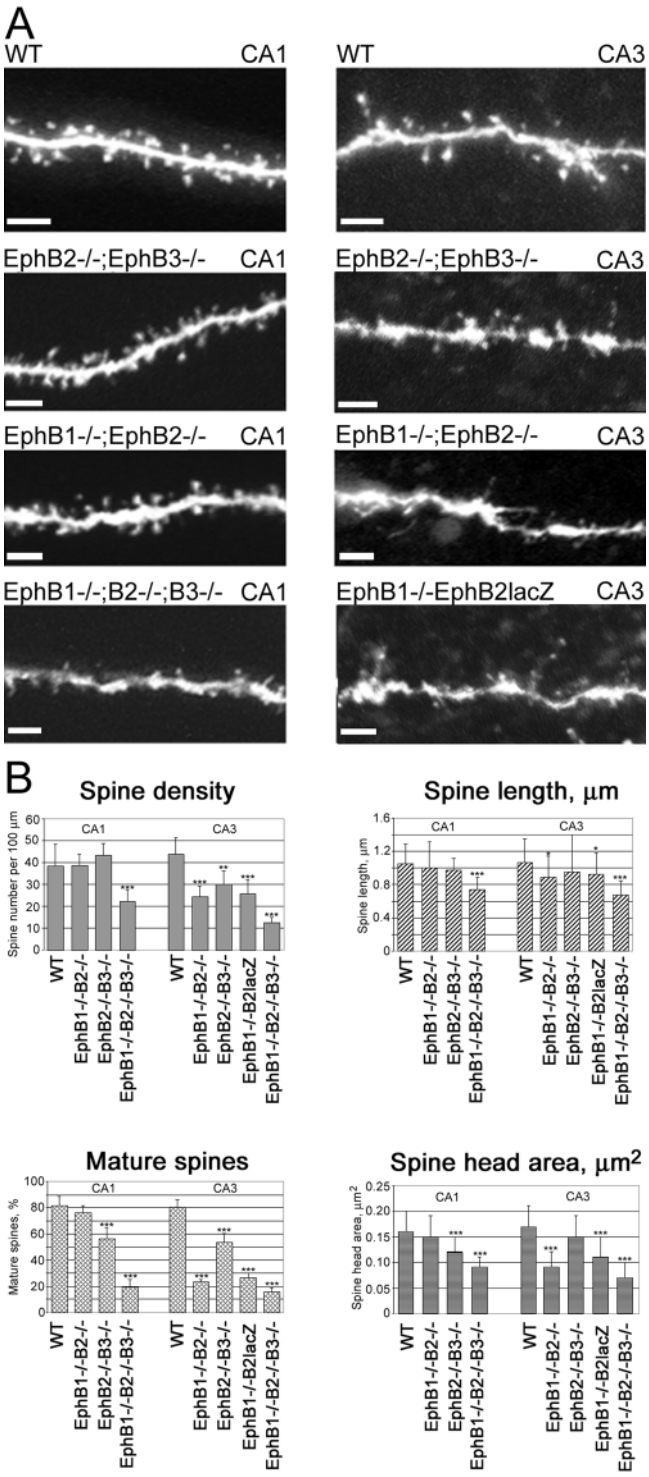

Figure 7. **Multiple EphB receptors are responsible for spine morphogenesis in hippocampus in vivo.** (A) Spine morphology in biocytin-filled CA1 and CA3 neurons of hippocampal slices from WT and EphB-deficient mice: double EphB KOs (EphB1−/−;EphB2−/−, or EphB2−/−;EphB3−/−); triple EphB KO (EphB1−/−;EphB2−/−; EphB3−/−), or mutant that express a truncated form of the EphB2 (EphB2−/−;EphB2lacZ). Bars, 2 µm. (B) Quantifications of spine density (top, left), spine lengths (top, right), percent of mature spines relative to total number of protrusions (bottom, left), and spine head area (bottom, right). Mature spines are defined as mushroom-shaped spines with large heads or stubby spines. Error bars indicate SD. *, $P < 0.05$; **, $P < 0.001$; ***, $P < 0.0001$ with *t* test.

served in vitro. However, in vivo the lack of spines is not compensated by extension of new filopodia. Although in vitro a low number of synaptic contacts results in the reformation of new filopodia in an attempt to build new synapses, in vivo astrocytic processes infiltrate vacant spaces where synaptic contact fail to establish and prevent extension of new filopodia (Fig. 9). Ephrin-A/EphA4 signaling that remains in triple EphB-deficient neurons could also contribute to the glia-restricted extension of new filopodia.

Our data suggest that although the EphA receptors are involved in glia-dependent control of filopodia extension and stabilization of spines, the EphBs play an important role in the axon–dendritic course of spine formation in hippocampal neurons both in vivo and in vitro.

The EphB receptors control spine morphogenesis

Beside the role of EphBs in spine formation, they also control spine maturation. Both the disruption of the EphB expression and inhibition of their kinase activity impair formation of mature mushroom-like spines in hippocampal neurons in vitro and in vivo. Although in absence of EphBs, EphAs may help control spine length and promote spine formation, although at much smaller rate, the presence of EphAs does not support spine maturation. The few spines that form in the hippocampi of triple EphB-deficient neurons in vivo have immature, headless or small-headed morphology (Figs. 6–8). Moreover, in vitro ephrin-B2–mediated activation of the EphBs in WT hippocampal neurons transforms thin immature spines into mature forms with spacious spine heads. Although ephrin-B2 treatment of the triple EphB-deficient hippocampal neurons does not promote spine morphogenesis.

Changes in spine morphology have been widely used as an indicator of synapse formation and function. It is likely that the robust changes in spine morphology, synapse number and synapse ultrastructure that are seen in hippocampi of the multiple EphB KOs would also affect synaptic function, especially considering that the defects in hippocampal LTP were already seen after a single EphB2 deletion (Grunwald et al., 2001). The asymmetric synapses are typically formed on spine heads and their size directly correlates with size of the synapse (Harris and Kater, 1994). PSD-95 promotes assembly of a postsynaptic complex, including NMDAR and AMPAR recruitment (Craven and Bredt, 1998), that directly correlates with formation of spacious spine heads (Ziv and Garner, 2001). Our data reveal that small-headed spines in hippocampi of triple EphB-deficient mice also have smaller PSDs and decreased PSD-95 IR (Fig. 6 D and Fig. 8). Moreover, the ephrin-B2–mediated activation of the EphBs promotes spine morphogenesis that consists of spine head formation and enlargement. How do the EphBs control spine morphogenesis?

There are several other proteins that have been shown to induce mature spine morphology, such as Syndecan-2 (Ethell and Yamaguchi, 1999), SPAR (Pak et al., 2001), Kalirin-7 (Penzes et al., 2001), Shank, Homer (Sala et al., 2001), and LIMK (Meng et al., 2002). Although all of them induce enlargement of spine heads, their additional effects on spines are different dependent on the protein that is involved, such as formation of aberrant spines induced by Kalirin-7 or spine complexity induced by SPAR. The EphB2 has been shown to regulate syndecan-2– and Kalirin-7–mediated spine morpho-

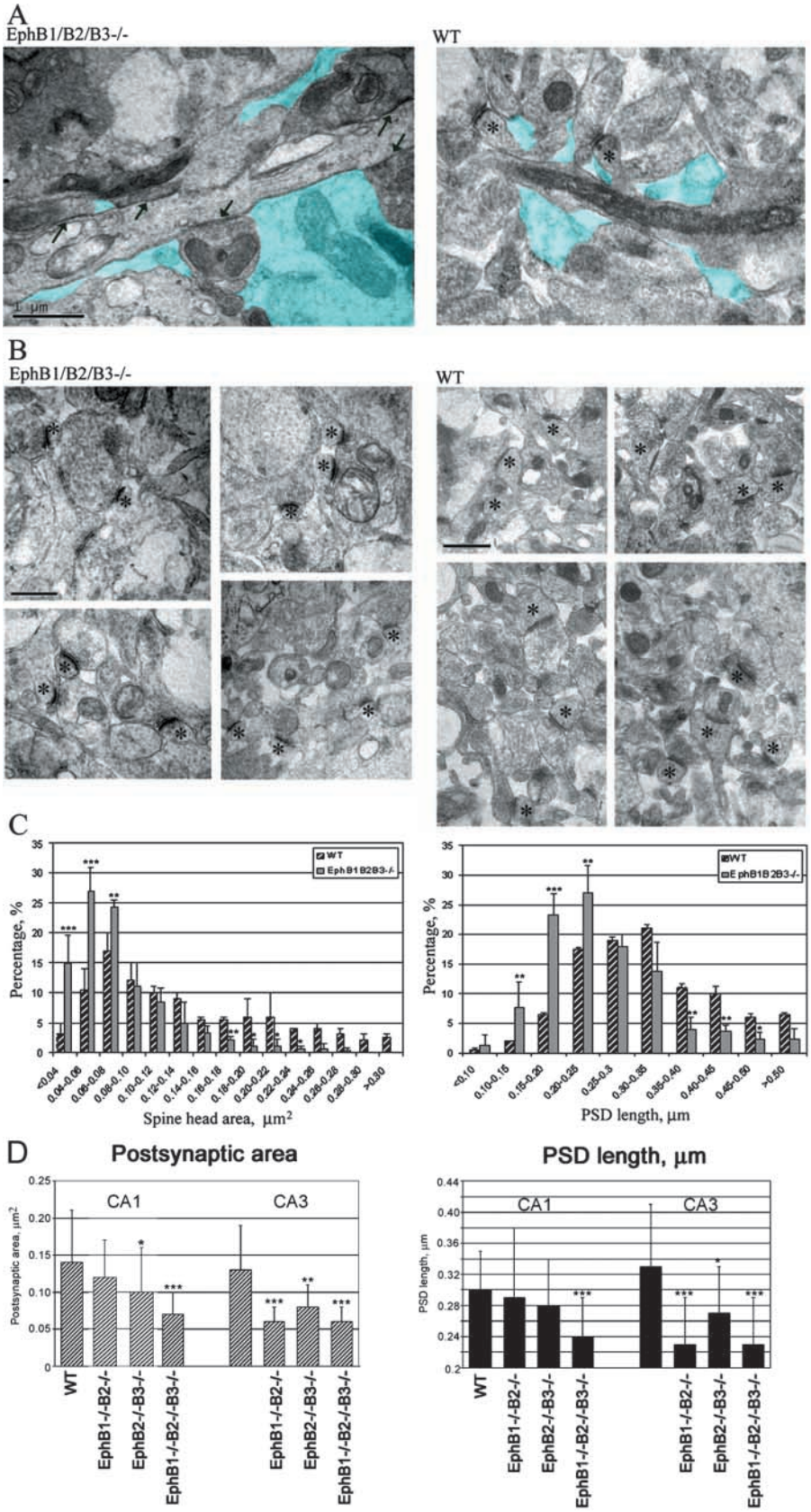

Figure 8. **The post-synaptic component and PSD area of asymmetric synapses (spines) are significantly reduced in the triple EphB-deficient hippocampus.** Representative electron micrographs of ultrathin sections of CA3 hippocampus from triple EphB-deficient (EphB1B2B3−/−) or WT mice. (A) Representative electron micrograph of longitudinal section through the dendrite shows increased number of symmetric synapses on dendritic shaft (arrows) in triple EphB-deficient neurons (EphB1B2B3−/−), as compared with WT. Note: The dendrite is ensheathed by astrocytic processes (blue). Bar, 1 µm. (B) Representative electron micrographs that show cross-sectional areas of post-synaptic component (asterisks) and PSD of asymmetric synapses in CA3 hippocampus of triple EphB-deficient (EphB1B2B3−/−) or WT mice. Bars, 1 µm. (C) Quantification of cross-sectional area of post-synaptic component (left) and PSD area (right) of asymmetric synapses (spines) in hippocampi of triple EphB-deficient (EphB1B2B3−/−) and WT mice. (D) Quantification of cross-sectional area of post-synaptic component (left, post-synaptic area) and PSD length of asymmetric synapses (right) in CA1 and CA3 areas of hippocampi from WT and the EphB-deficient mice: double EphB KOs (EphB1−/−; EphB2−/−, or EphB2−/−;EphB3−/−); and triple EphB KO (EphB1−/−; EphB2−/−; EphB3−/−). (C and D) Error bars indicate SD. *, $P < 0.05$; **, $P < 0.001$; ***, $P < 0.0001$ with *t* test.

genesis in cultured hippocampal neurons by recruitment of these proteins to post-synaptic sites (Ethell et al., 2001; Penzes et al., 2003). Although, the relationship between EphB signaling and SPAR or LIMK is unclear, LIMK, which is a downstream target of Rac1 and Pak, may be affected by the Rho-GEF activity of Kalirin-7. Clearly there are multiple

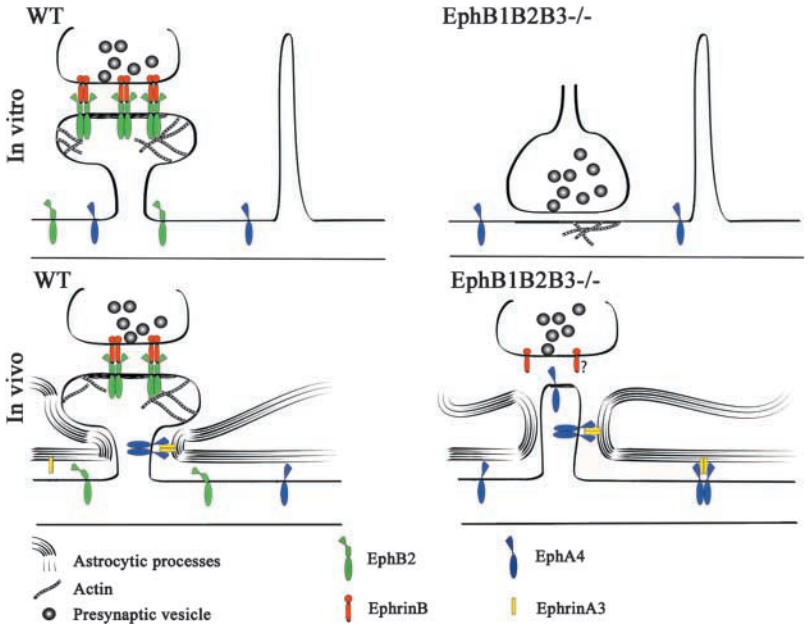

Figure 9. **Schematic representation of spines in triple EphB-deficient hippocampal neurons in vitro and in vivo.** In vitro, *WT* hippocampal neurons form spines with asymmetric synapses and large heads containing polymerized actin and large PSD. The dendrites are not ensheathed by astrocytic processes. Small number of filopodia is found in mature neurons. In vitro, *triple EphB1B2B3 −/−* hippocampal neurons don't form spines. There are many filopodia are formed and only symmetric synapses on dendritic shaft are found. The dendrites are not ensheathed by astrocytic processes. In vivo, *WT* hippocampal neurons form spines with asymmetric synapses, bulbous heads, and large PSD. The dendrites and synapses are enwrapped by astrocytic processes. Filopodia are usually not found in mature neurons. In vivo, *triple EphB1B2B3 −/−* hippocampal neurons form fewer spines. These spines have immature small-headed or headless morphology and reduced PSD length. The dendrites and synapses are enwrapped by astrocytic processes. Small number of filopodia is found in mature neurons.

proteins that control spine morphogenesis and whether they converge on a common molecular mechanisms remains to be further explored. Nevertheless, all of the proteins that have been shown to be involved in spine morphogenesis, including scaffolding proteins (Syndecan-2, Shank, Homer), and signal transduction proteins (SPAR, LIMK Kalirin-7), directly or indirectly regulate rearrangements of actin cytoskeleton that are responsible for spine morphogenesis.

The EphB receptor regulation of actin cytoskeleton in spines

The triple EphB-deficient hippocampal neurons show abnormal formation of actin clusters along the dendrites avoiding spines, whereas in WT neurons, spine maturation directly correlates with actin accumulation in spines (Fig. 2 A). The actin filament accumulation in spines is disrupted in the KO neurons indicating that the EphB responsible for targeting of actin to spines.

Dynamic reorganization of the actin cytoskeleton is an important step underlying morphological changes in spines during their formation and maturation. Members of the Rho family of small GTPases (RhoA, Rac and CDC-42) have been reported to play a role in maintaining spine morphology in mature hippocampal neurons in vitro (Nakayama et al., 2000). Most recently, two groups have shown that Ephrin-B–mediated activation of EphBs induces activation of Rac1 and Cdc42 through the translocation of the Rho-GEF factors Kalirin and Intersectin, respectively, to post-synaptic sites of hippocampal neurons (Irie and Yamaguchi, 2002; Penzes et al., 2003). Altogether, these data suggest that EphB-mediated activation of small RhoGTPases contributes to ephrin-B effects on spine morphological features, such as filopodia shrinkage and the formation of stable, mature, mushroom-like spines. The deletion of EphBs did not effect actin polymerization or the formation of branched F-actin, but rather prevented the targeting of F-actin to dendritic protrusions and their transformation to spines. Therefore, the temporal and spatial switch between different Rho GTPases might be critical in RhoGTPase-dependent spine morphogenesis. More investigation is needed to determine whether EphBs are key regulators of the balance between different RhoGTPase activities in spines that drives spine morphogenesis.

Materials and methods

Mice

The triple homozygotes were generated using protein-null mutation in the EphB1 gene (Williams et al., 2003), and null mutations in EphB2 (Henkemeyer et al., 1996) and EphB3 (Orioli et al., 1996).

Hippocampal neuron culture, transfection

Cultures of mouse hippocampal neurons were prepared from mouse E15-16 embryos (WT and mutant) as described previously with modifications (Ethell et al., 2001). The hippocampal neuron cultures were transiently transfected with GFP at 5–7 DIV as described previously (Ethell and Yamaguchi, 1999). Transfected neurons have been shown to express significant level of GFP for 20 d after transfection.

Immunostaining

The GFP-transfected cultures of hippocampal neurons at 21 DIV were fixed in 2% PFA. The spine morphology was visualized by GFP fluorescence and analyzed quantitatively as described previously (Ethell and Yamaguchi, 1999). To detect polymerized F-actin, the fixed cells were incubated with the rhodamine-coupled phalloidin (1:40, R-415, Molecular Probes). To analyze synapse formation and localization of ephrins-B and EphBs, the fixed cells were treated with 0.1% Triton X-100 and blocked with 5% NGS containing 1% BSA. The primary antibodies used were: 2 μg/ml rabbit anti-EphB2 (a gift from E. Pasquale [The Burnham Institute, La Jolla, CA] used previously in Ethell et al., 2001); 2 μg/ml goat anti-EphB1 (M19; Santa Cruz Biotechnology, Inc.); 1 μg/ml goat anti-EphB3 (R&D Systems); 4 μg/ml rabbit anti–pan-ephrin-B (C18; Santa Cruz Biotechnology, Inc.); mouse anti-synaptophysin (SVP-38; Sigma-Aldrich); mouse anti-neurofilament 200 (clone NE14; Sigma-Aldrich); mouse anti–PSD-95 (clone 6G6; Affinity BioReagents, Inc.); 10 μg/ml mouse anti-GluR2 (MAB397; CHEMICON International Inc.); 1 μg/ml rabbit anti-NMDAR2A/B (AB1548; CHEMICON International, Inc.); and 5 μg/ml mouse anti-GAD (GAD65; BD Biosciences) antibodies. The secondary antibodies used were: 1 μg/ml FITC-conjugated donkey anti–goat IgG (Santa Cruz Biotechnology, Inc.); 4 μg/ml Alexa Fluor 594–conjugated donkey anti–rabbit IgG (Molecular Probes); 4 μg/ml Alexa 488–conjugated goat anti–rabbit IgG (Molecular Probes); and 4 μg/ml Alexa 594–conjugated goat anti–mouse IgG (Molecular Probes). Immunostaining was analyzed under a confocal laser scanning microscope (model LSM 510; Carl Zeiss MicroImaging, Inc.).

Imaging and image analysis

To activate the EphBs in cultured hippocampal neurons, we used ephrinB2-Fc (R&D Systems), preclustered with anti–human Fc antibody (Jackson ImmunoResearch Laboratories) before the application. To precluster, ephrin-B2-Fc was mixed with anti–human Fc antibody in a 1:2 ratio and incubated on ice for 1 h before being applied to the cultured neurons.

To examine spine formation, we monitored morphology of dendritic protrusions in 7 DIV GFP-expressed neurons before and after the application of preclustered ephrin-B2-Fc or control preclustered Fc in concentration of 2 μg/ml (Jackson ImmunoResearch Laboratories) The time-lapse imaging was performed on an inverted fluorescent microscope (model TE300; Nikon) with a 40X air or 63X/1.40 oil Fluor objectives and monitored by 12-bit CCD camera (model Orca-100; Hamamatsu) using MetaFluor/MetaMoph software (Universal Imaging Corp.) running on a Pentium-II based computer. The cultures were maintained at 37°C during the whole experiment in HBSS on Warner thermostated stage, and images were captured at 5-min intervals for 30 min after application of clustered ephrin-B2-Fc or control Fc.

The effect of EphB activation on spine maturation was examined in 14 DIV GFP-expressing hippocampal neurons. The preclustered ephrin-B2-Fc was applied to the 14 DIV cultures. After 4 h of treatment, cultured hippocampal neurons were fixed in 2% PFA and analyzed by immunostaining.

Immunohistochemistry

Immunohistochemistry was performed on frozen sections. In brief, adult mice were deeply anesthetized with pentobarbital (~0.3 mg), and perfused transcardially with ice-cold 0.9% saline followed by fixation in 4% PFA. Whole brains were dissected, immersed in 30% sucrose in PBS overnight at 4 C, frozen on dry ice, and embedded in OCT compound (Miles). 10-mm-thick coronal sections were cut on cryostat. Before immunostaining, the sections were rehydrated in PBS at RT, permeabilized with 0.1% Triton X-100, and blocked in 5% NGS with 1% BSA. Primary antibodies were mouse anti–PSD-95 (clone 6G6; ABR) and mouse anti-synaptophysin (clone SVP-38; Sigma-Aldrich), applied in combinations with 1.6 μg/ml rabbit anti-calbindin antibody (CHEMICON International, Inc.). The secondary antibodies were 4 μg/ml Alexa Flour 594–conjugated goat anti–mouse IgG (Molecular Probes) and 4 μg/ml Alexa Flour 488–conjugated goat anti–rabbit IgG (Molecular Probes). Immunostaining was analyzed under a confocal laser scanning microscope (model LSM 510; Carl Zeiss MicroImaging, Inc.).

Biochemical assays

Brain tissues or cultured hippocampal neurons were lysed in ice-cold TBS (25 mM Tris, pH 7.4, 0.15 mM NaCl) containing 1% Triton X-100, 5 mM EDTA, 0.5 mM pervanadate, and protease inhibitor cocktail (Sigma-Aldrich). Cell lysates were cleared by centrifugation at 14,000 rpm. Protein concentration was determined using the BCA Protein Assay kit (Pierce Chemical Co.). The proteins were resolved on an 8–16% Tris-glycine gels (30 μg of total protein per sample) and transferred onto nitrocellulose membranes. The EphBs were detected using one of the following antibodies: 1 μg/ml anti-EphB1 (Santa Cruz Biotechnology, Inc.); 0.1 μg/ml anti-EphB2 (R&D Systems); and 0.1 μg/ml anti-EphB3 (R&D Systems); and secondary HRP-conjugated donkey anti–goat IgG (Jackson ImmunoResearch Laboratories) with Super Signal West Pico chemiluminescent substrate (Pierce Chemical Co.).

For immunoprecipitation, cultured hippocampal neurons were treated with 2 μg/ml preclustered ephrin-B2-Fc or control Fc for 15 min, and cell lysates were prepared as described in the previous paragraph. The lysates were incubated with rabbit anti-EphB2 antibody (a gift from E. Pasquale, used previously in Ethell et al., 2001) and protein A–Sepharose (Sigma-Aldrich) for 2 h at 4°C. The beads were washed five times with TBS. The bound materials were eluted with SDS-PAGE sample buffer, resolved on an 8–16% Tris-glycine gels and immunoblotted with HRP-conjugated anti-phosphotyrosine antibody (PY20; BD Transduction Laboratories).

Subcellular fractionations of cultured hippocampal neurons were prepared from 21-d-old cultures as described previously (Ethell et al., 2000). The cell homogenates, soluble, crude synaptosome, and synaptic membrane fractions were analyzed by immunoblotting with mouse anti–PSD-95 (clone 6G6; ABR), mouse anti-synaptophysin (clone SVP-38; Sigma-Aldrich), mouse anti-GluR2 (CHEMICON International, Inc.), and rabbit anti-NMDAR2A/B antibodies (CHEMICON International, Inc.).

Slices

Mice were deeply anesthetized with ~0.3 mg pentobarbital and decapitated. The brains were rapidly removed, and 300-μm-thick coronal slices of one hemisphere were cut. Slices containing transverse sections of hippocampus were maintained in standard mammalian bicarbonate buffer. Neurons for biocytin filling were obtained using blind whole-cell recording (Blanton et al., 1989) from the CA1 and CA3 regions of the hippocampus as described previously (Hickmott and Merzenich, 2002). Morphology of spines was analyzed under a confocal laser scanning microscope (model LSM 510; Carl Zeiss MicroImaging, Inc.). Serial optical sections were taken at 0.5-μm intervals in X-Y plane. The three-dimensional fluorescent images were created as a result of projection of the optical serial sections.

Electron microscopy

The coronal brain slices containing transverse sections of hippocampi (as described in Slices) were fixed in 2% glutaraldehyde in PBS for 2 h, fixed after in 1% osmium tetroxide in PBS for 2 h, and proceeded for EM as described previously (Ethell et al., 2000). In brief, the hippocampal slices were cut into small pieces, dehydrated with ethanol, and embedded in Spurr resin. Ultrathin sections were cut on a RMC MT-X ultra microtome and stained after with uranyl acetate and lead citrate. The sections were viewed in a transmission electron microscope (model Tecnai 12; FEI Company).

Data analysis

All quantitative measurements were performed using MetaMorph and Scion image softwares. Statistical analysis was performed using Microsoft Excel as described previously (Ethell and Yamaguchi, 1999). Groups of spines were compared with *t* test.

Online supplemental material

Clustered ephrin-B2-Fc promotes spine morphogenesis in 7 DIV–cultured hippocampal neurons (Fig. S1). Clustered ephrin-B2-Fc or control Fc was applied to cultured GFP-expressing hippocampal neurons at 7 DIV. The morphology of protrusions was visualized by GFP and live images were captured at 5-min intervals for 30 min. The online supplemental material is available at http://www.jcb.org/cgi/content/full/jcb.200306033/DC1.

We thank Dr. Elena Pasquale for her gift of antibodies and reagents, Stephen McDaniel for technical assistance with EM, Dr. Patricia Steen for her help on confocal imaging, Dr. Christian Lytle for his advice on time-lapse imaging, and Dr. Elena Pasquale and Dr. Mike Moeller for helpful discussion and critical reading of the manuscript.

This work was supported by the National Institutes of Health grants MH67121 (to I. Ethell), MH66332 (to M. Henkemeyer), and NS42241 (to P. Hickmott), and by the March of Dimes Birth Defects Foundation (to M. Henkemeyer).

Submitted: 6 June 2003
Accepted: 7 November 2003

References

Blanton, M.G., J.J. Lo Turco, and A.R. Kriegstein. 1989. Whole cell recording from neurons in slices of reptilian and mammalian cerebral cortex. *J. Neurosci. Methods.* 30:203–210.

Buchert, M., S. Schneider, V. Meskenaite, M.T. Adams, E. Canaani, T. Baechi, K. Moelling, and C.M. Hovens. 1999. The junction-associated protein AF-6 interacts and clusters with specific Eph receptor tyrosine kinases at specialized sites of cell–cell contact in the brain. *J. Cell Biol.* 144:361–371.

Cowan, C.A., and M. Henkemeyer. 2002. Ephrins in reverse, park, and drive. *Trends Cell Biol.* 12:339–346.

Craven, S.E., and D.S. Bredt. 1998. PDZ proteins organize synaptic signaling pathways. *Cell.* 93:495–498.

Dalva, M.B., M.A. Takasu, M.Z. Lin, S.M. Shamah, L. Hu, N.W. Gale, and M.E. Greenberg. 2000. EphBs interact with NMDA receptors and regulate excitatory synapse formation. *Cell.* 103:945–956.

Ethell, I.M., and Y. Yamaguchi. 1999. Cell surface heparan sulfate proteoglycan syndecan-2 induces the maturation of spines in rat hippocampal neurons. *J. Cell Biol.* 144:575–586.

Ethell, I.M., K. Hagihara, Y. Miura, F. Irie, and Y. Yamaguchi. 2000. Synbindin, a novel syndecan-2–binding protein in neuronal dendritic spines. *J. Cell Biol.* 151:53–67.

Ethell, I.M., F. Irie, M.S. Kalo, J.R. Couchman, E.B. Pasquale, and Y. Yamaguchi. 2001. EphB/syndecan-2 signaling in dendritic spine morphogenesis. *Neuron.* 31:1001–1013.

Fiala, J.C., J. Spacek, and K.M. Harris. 2002. Dendritic spine pathology: cause or consequence of neurological disorders? *Brain Res. Brain Res. Rev.* 39:29–54.

Flanagan, J.G., and P. Vanderhaeghen. 1998. The ephrins and Eph receptors in

neural development. *Annu. Rev. Neurosci.* 21:309–345.

Gerlai, R. 2000. Protein targeting: altering receptor kinase function in the brain. *Trends Neurosci.* 23:236–239.

Grunwald, I.C., M. Korte, D. Wolfer, G.A. Wilkinson, K. Unsicker, H.P. Lipp, T. Bonhoeffer, and R. Klein. 2001. Kinase-independent requirement of EphB2 receptors in hippocampal synaptic plasticity. *Neuron.* 32:1027–1040.

Harris, K.M., and S.B. Kater. 1994. Dendritic spines: cellular specializations imparting both stability and flexibility to synaptic function. *Annu. Rev. Neurosci.* 17:341–371.

Harris, K.M. 1999. Structure, development, and plasticity of dendritic spines. *Curr. Opin. Neurobiol.* 9:343–348.

Henderson, J.T., J. Georgiou, Z. Jia, J. Robertson, S. Elowe, J.C. Roder, and T. Pawson. 2001. The receptor tyrosine kinase EphB2 regulates NMDA-dependent synaptic function. *Neuron.* 32:1041–1056.

Henkemeyer, M., D. Orioli, J.T. Henderson, T.M. Saxton, J. Roder, T. Pawson, and R. Klein. 1996. Nuk controls pathfinding of commissural axons in the mammalian central nervous system. *Cell.* 86:35–46.

Hickmott, P.W., and M.M. Merzenich. 2002. Local circuit properties underlying cortical reorganization. *J. Neurophysiol.* 88:1288–1301.

Irie, F., and Y. Yamaguchi. 2002. EphB receptors regulate dendritic spine development via intersectin, Cdc42 and N-WASP. *Nat. Neurosci.* 5:1117–1118.

Irwin, S.A., B. Patel, M. Idupulapati, J.B. Harris, R.A. Crisostomo, B.P. Larsen, F. Kooy, P.J. Willems, P. Cras, P.B. Kozlowski, et al. 2001. Abnormal dendritic spine characteristics in the temporal and visual cortices of patients with fragile-X syndrome: a quantitative examination. *Am. J. Med. Genet.* 98:161–167.

Kaufmann, W.E., and H.W. Moser. 2000. Dendritic abnormalities in disorders associated with mental retardation. *Cereb. Cortex.* 10:981–991.

Kullander, K., and R. Klein. 2002. Mechanisms and functions of Eph and ephrin signaling. *Nat. Rev. Mol. Cell Biol.* 3:475–486.

Liebl, D.J., C.J. Morris, M. Henkemeyer, and L.F. Parada. 2003. mRNA expression of ephrins and Eph receptor tyrosine kinases in the neonatal and adult mouse central nervous system. *J. Neurosci. Res.* 71:7–22.

Meng, Y., Y. Zhang, V. Tregoubov, C. Janus, L. Cruz, M. Jackson, W.Y. Lu, J.F. MacDonald, J.Y. Wang, D.L. Falls, and Z. Jia. 2002. Abnormal spine morphology and enhanced LTP in LIMK-1 knockout mice. *Neuron.* 35:121–133.

Murai, K.K., L.N. Nguyen, F. Irie, Y. Yamaguchi, and E.B. Pasquale. 2003. Control of hippocampal dendritic spine morphology through ephrin-A3/EphA4 signaling. *Nat. Neurosci.* 6:153–160.

Nakayama, A.Y., M.B. Harms, and L. Luo. 2000. Small GTPases Rac and Rho in the maintenance of dendritic spines and branches in hippocampal pyramidal neurons. *J. Neurosci.* 20:5329–5338.

Orioli, D., M. Henkemeyer, G. Lemke, R. Klein, and T. Pawson. 1996. Sek4 and Nuk receptors cooperate in guidance of commissural axons and in palate formation. *EMBO J.* 15:6035–6049.

Pak, D.T., S. Yang, S. Rudolph-Correia, E. Kimand, and M. Sheng. 2001. Regulation of dendritic spine morphology by SPAR, a PSD-95-associated RapGAP. *Neuron.* 31:289–303.

Pasquale, E.B. 1997. The Eph family of receptors. *Curr. Opin. Cell Biol.* 9:608–615.

Penzes, P., R.C. Johnson, R. Sattler, X. Zhang, R.L. Huganir, V. Kambampati, R.E. Mains, and B.A. Eipper. 2001. The neuronal Rho-GEF Kalirin-7 interacts with PDZ domain-containing proteins and regulates dendritic morphogenesis. *Neuron.* 29:229–242.

Penzes, P., A. Beeser, J. Chernoff, M.R. Schiller, B.A. Eipper, R.E. Mains, and R.L. Huganir. 2003. Rapid induction of dendritic spine morphogenesis by trans-synaptic ephrinB-EphB receptor activation of the Rho-GEF kalirin. *Neuron.* 37:263–274.

Sala, C., V. Piech, N.R. Wilson, M. Passafaro, G. Liu, and M. Sheng. 2001. Regulation of dendritic spine morphology and synaptic function by Shank and Homer. *Neuron.* 31:115–130.

Torres, R., B.L. Firestein, H. Dong, J. Staudinger, E.N. Olson, R.L. Huganir, D.S. Bredt, N.W. Gale, and G.D. Yancopoulos. 1998. PDZ proteins bind, cluster, and synaptically colocalize with Eph receptors and their ephrin ligands. *Neuron.* 21:1453–1463.

Williams, S.E., F. Mann, L. Erskine, T. Sakurai, S. Wei, D.J. Rossi, N.W. Gale, C.E. Holt, C.A. Mason, and M. Henkemeyer. 2003. Ephrin-B2 and EphB1 mediate retinal axon divergence at the optic chiasm. *Neuron.* 39:919–935.

Ziv, N.E., and C.C. Garner. 2001. Principles of glutamatergic synapse formation: seeing the forest for the trees. *Curr. Opin. Neurobiol.* 11:536–543.